Desalination and Water Treatment
www.deswater.com
doi: 10.1080/19443994.2014.910137

54 (2015) 3257–3268
June

Taylor & Francis
Taylor & Francis Group

Preparation and characterisation of PES-ZnO mixed matrix membranes for humic acid removal

A.L. Ahmad[a,*], A.A. Abdulkarim[a,b], S. Ismail[a], B.S. Ooi[a]

[a]*School of Chemical Engineering, Engineering Campus, Universiti Sains Malaysia, Nibong Tebal 14300, Penang, Malaysia, Tel. +60 45995999; Fax: +60 45941013; email: chlatif@eng.usm.my*
[b]*Chemical and Petrochemical Research Center, Commission for Research and Industrial Development, Ministry of Industry and Minerals, Baghdad, Iraq*

Received 2 October 2013; Accepted 23 March 2014

ABSTRACT

Zinc oxide nanoparticles (ZnO-NPs) were incorporated into polyethersulfone (PES) matrix to prepare mixed matrix membranes. The separation performance of mixed matrix membranes with respect to humic acid (HA) removal was significantly improved through the addition of ZnO-NPs. The membranes were synthesised by dispersing various amounts of hydrophilic ZnO-NPs (0–3.75 wt.%) into a dope solution containing PES, polyvinylpyrrolidone (PVP) and dimethylacetamide in the appropriate proportions. SEM and AFM were employed to investigate the dispersion of the ZnO-NPs within the polymer matrix and characterise the surface properties of the particles. The pure water flux, HA flux and rejection rate, and the fouling resistance were investigated to evaluate the membrane performance. The characterisation results indicated that all of the PES/ZnO membranes possessed a smaller pore size than that of the pristine PES membrane. The HA rejection rates were observed to increase with the amount of added ZnO. In particular, the PES/ZnO membrane with 1.25 wt.% ZnO exhibited the highest pure water and HA fluxes. Additionally, the fouling analysis revealed that all of the PES/ZnO membranes exhibited a decrease in their HA fouling tendency.

Keywords: Membrane; Water treatment; Zinc oxide; Nanoparticles; Humic acid

1. Introduction

The soaring world population has led to an increase in the demand for drinking water, the quality of which has become the foremost issue of this era. Thus, the academic and the industrial community have devoted serious attention to defining the relevant problems surrounding this issue and their solution to furnish high-quality drinking water. Recently, research concerning membrane technologies for the purification of drinking water has been undertaken. The performance measure of such technologies is the extent to which natural organic matter (NOM) is removed [1,2]. It is well established that the presence of NOM in aquatic resources is not harmful, but concern arises if such water is treated with chlorine in the disinfection step. The presence of organic matter, such as humic acid (HA) and fulvic acid (FA), may lead to the formation of chlorinated by-products in drinking water via their reaction with organic compounds. Trihalomethane and haloacetic acids are good examples of such

*Corresponding author.

by-products and are considered carcinogenic [3]. In nature, the mixture of these acids (HA and FA) is heterogeneous and possesses three main functional groups, i.e. carboxylic acid (COOH), phenolic alcohols (OH) and methoxy carbonyls (C=O) [4]. It is widely reported that HA is considered a model compound for the investigation of membrane efficacy in water treatment applications [1,5].

Polyethersulfone (PES) is one of the most important polymeric materials applied in water treatment membranes [6,7]. The knowledge of glass transition temperature (T_g) is essential in the selection of polymeric materials, which could be defined as the temperature at which an amorphous polymer becomes soft upon heating or brittle upon cooling. The measurement of polymer T_g could help in the evaluation of the rigidity and the excess free volume of the polymer [8], also it gives an indication about the miscibility of the polymer with the additive. The high T_g (225˚C) and amorphous nature [9] are the main attractive characteristics of PES, which make it applicable in the preparation of asymmetric membranes with different pore sizes and varying surface geometry [9–11]. However, PES-based membranes often cause serious fouling when applied in water treatment due to their hydrophobicity.

One of the possible ways to improve the membrane fouling resistance of PES membranes is by increasing their hydrophilicity. It is reported that the incorporation of inorganic materials into a PES membrane matrix may improve the hydrophilicity [2,12–16]. Adding nanoparticles (NPs) to PES membranes may potentially enhance the membranes' structure and improve their separation performance, which can be attributed to the stable physical properties of NPs, such as high surface area and thermal/mechanical stability. The fabrication of membranes with high fouling resistance can be achieved using these particles. Indeed, the improved fouling resistance of such membranes may be ascribed to the functional groups as well as the hydrophilic characteristics of these particles [17]. One of the crucial issues in the preparation of mixed matrix membranes is the dispersion of the NPs. Improper distribution of these NPs in the membrane matrix leads to decrease in performance and affect the surface characteristics of these membranes. In addition to the mechanical dispersion of NPs, the incorporation of chemicals such as polyethylene glycol (PEG) [18], polyvinylpyrrolidone (PVP) [1] and polyvinyl alcohol [19] in the dope solution has been used to improve the dispersion of various types of NPs such as TiO_2 and ZnO.

ZnO-NPs have garnered special attention due to their low cost, superior surface area, photo-catalytic activity and anti-bacterial properties [20–22]. In several studies, ZnO-NPs have been incorporated into different membrane materials and have led to improved performance [18,19,23–26]. Leo et al. [19] improved the hydrophilicity of polysulfone membranes by incorporating 1–4 wt.% ZnO-NPs and polyvinyl alcohol. The authors observed a 12-fold improvement in membrane permeability due to presence of ZnO-NPs (2 wt.%) in polysulfone membranes. Moreover, this type of membrane exhibited the highest fouling resistance during oleic acid filtration. Balta et al. [24] used high PES concentrations (25–32 wt.%) with a wide range of ZnO-NP concentrations (0.035–4 wt.%) to develop a mixed matrix membrane. The authors observed a significant improvement in water permeability as well as HA rejection. However, at high-polymer concentration, the composite membrane showed decrease in permeability due to a reduction in the NP dispersion rate. Additionally, Shen and co-workers [18] reported the dispersion of ZnO-NPs (0.199–0.793 wt.%) in a solvent using a low concentration of PES (15.87–16 wt.%) and PEG. The researchers claimed that the membrane hydrophilicity increased, as the ZnO concentration increased. Moreover, the membrane permeability was improved by 254% (obtained at 0.398 wt.% ZnO-NPs) relative to that of a pristine PES membrane.

To the best of our knowledge, formulation of mixed matrix membrane containing high ZnO-NPs to PES ratio was not yet reported. Therefore, the aim of the present work is to develop the high ZnO content nanocomposite membranes with the aid of PVP as a dispersing agent. Emphasis was placed on the method of preparation and performance assessment of the mixed matrix membranes in HA removal. In addition, the prepared mixed matrix membranes were characterised using scanning electron microscopy (SEM), atomic force microscopy (AFM), contact-angle, membrane filtration experiments and fouling analysis.

2. Experiment

2.1. Materials

Polyethersulfone (PES Ultrason E6020P with Mw = 58,000 g/mol) was supplied from BASF. PVP (with Mw = 40,000 g/mol), sodium hydroxide, HA and N,N-dimethylacetamide (DMAc), as a solvent, were supplied from Sigma Aldrich (USA). A commercial form of zinc oxide NPs, ZnO nanopowder (particle size range of 10–30 nm; purity > 99%), was supplied by US Research Nanomaterials, Inc. (Houston, TX).

2.2. Preparation of PES/ZnO composite membranes

Flat-sheet composite membranes were prepared by phase inversion via the immersion precipitation

technique. Membrane solutions were prepared by dispersing varying amounts of NPs (ranging from 0 to 3.75 wt.%) in DMAc solvent (ranging from 76.75 to 80.5 wt.%). The solutions were mechanically stirred (600 rpm) at room temperature for 3 h. Then, the mixtures were ultrasonicated for 10 min and stirred for 3 h. Subsequently, the appropriate amount of PVP (corresponding to 3.75 wt.%) was added, and stirring was continued for another 5 h. A calculated amount of PES polymer (corresponding to 15.75 wt.%) was then added over a period of 2 h, and the mixture solutions were kept under mechanical stirring (500 rpm) at 60˚C for 24 h. Table 1 presents the composition of the casting solution. To remove bubbles from the solutions, the homogeneous polymeric solutions were placed in an ultrasonic bath for 5 h. Each polymeric solution was cast with a casting knife measuring 200 μm in thickness onto a glass plate using a filmograph (K4340 automatic Film Applicator, Elcometer). Then, the membrane was exposed to air for 45 s, subsequently moved to a non-solvent bath (containing distilled water) at 20˚C and left for 24 h to allow for precipitation. The as-obtained membranes were thoroughly washed and stored at 25˚C in distilled water (DI) for 1 day to ensure the complete removal of the pre-used solvent and stored wet. For each polymeric solution composition, three identical membranes were prepared and tested to obtain an average value of the fluxes and HA solution rejection.

2.3. Membrane characterisation

2.3.1. SEM analysis

The surface morphologies of the prepared PES/ZnO membranes were studied by SEM using a HITACHI Tabletop Microscope instrument (TM-3000-Japan) operated at 20 kV. The morphology of cross-sectional area of all membranes was observed under field emission SEM (FESEM CARL ZEISS SUPRA 35VP, Germany). Membrane samples were cut into small sizes and mounted on a double-sided carbon adhesive foil as the sample holder. Prior to the SEM test, sputtered coating was used (Quorum-SC7620) to coat the membrane surface and cross-sectional area with a thin layer of gold under vacuum to avoid the effect of electrostatic charging.

Table 1
Composition of casting solutions (wt.%)

Membrane ID	PES	ZnO	PVP	DMAC
A1	15.75	0	3.75	80.5
A2	15.75	1.25	3.75	79.25
A3	15.75	2.5	3.75	78
A4	15.75	3.75	3.75	76.75

2.3.2. Atomic force microscopy

The surface roughness of the prepared membranes was investigated by AFM (Park System XE100, Korea). The membrane samples were observed at room temperature under tapping mode to obtain images with a scan size of 1 × 1 μm at a scan speed rate of 0.25 Hz. Roughness parameters such as the mean roughness (R_a), the standard deviation of the height in the scanned area (R_q) and the mean difference in height between the highest peaks and five lowest valleys (R_z) were obtained.

2.3.3. Contact-angle measurements

To evaluate the membranes' surface hydrophilicity, the contact angle between water and each membrane surface was directly measured using a contact-angle-measuring system (Rame-Hart 250-F1, USA). A water droplet (0.2 μL) was placed on a dry flat membrane surface, and the contact angle between the droplet and substrate was calculated. To reduce experimental error, the average value of a series of seven measurements for each membrane sample was considered.

2.3.4. Membrane pore size

The pore sizes of the membranes were determined via a gas flow/liquid displacement method using a Porolux 1,000 capillary flow porometer (Benelux Scientific, Belgium). Prior to testing, membrane samples with a diameter of 10 mm were immersed in perfluoroether (for 5 min) and then characterised using the "dry up-wet up" method. The mean pore size was then determined using LabView software.

The viscosity of dope solutions was measured using programmable Rheometer (Brookfield, USA) in a thermostatted oil bath at 26 ± 1˚C. The rotation speed was fixed at 15 rpm and the viscosities were measured after shearing for 30 s. For each polymer solution, the average of three viscosity values was obtained.

2.3.5. Filtration experiments

The membrane flux and separation performance of the prepared membranes were measured using a cross-flow filtration set-up [18]. All experiments were performed at an ambient laboratory temperature of 22 ± 1˚C. Typically, the experiments were conducted

through a cross-flow cell with an effective membrane area of 42 cm^2 and constant flow rate of 1,000 mL/min using a Flex-Pro-A4 V Peristaltic Metering Pump (Blue-White, USA). Initially, each of the tested membranes was compressed with pure water at 150 kPa for 1 h. The pure water flux measurement was performed at 100 kPa, and the flux was measured after 60 min of water filtration. A 5 L feed solution containing 10 mg/L (pH 7.7) of the HA solution was prepared and re-circulated at 100 kPa through the aforementioned cell. A HA solution was used to investigate membrane rejection and fouling. The HA concentration in the permeate was recorded after 60 min of the filtration experiment, fully recycling both the permeate and retentate in the process except during flux sampling.

The pure water flux (J_{WF}) was computed according to Eq. (1):

$$J_{WF} = \frac{V}{A * t} \tag{1}$$

where J_{WF} is the pure water flux (L/m^2 h), V is the permeate volume (L), A is the effective membrane surface area (m^2) and t is the measurement time (h).

The HA concentration in the feed and permeate flux were determined using a UV–vis spectrophotometer (Pharo 300, Merck-Germany) at a wavelength of 254 nm. As such, the membrane rejection was calculated according to Eq. (2):

$$\text{Rejection} = \left(1 - \frac{C_p}{C_f}\right) \times 100\% \tag{2}$$

where C_p (mg/L) and C_f (mg/L) represent the solute concentrations in the permeate and feed, respectively.

2.3.6. Membrane fouling analysis

The HA flux measurement was performed at 100 kPa for 180 min and at 22°C; this flux was recorded as J_{HA}. Then, each membrane was thoroughly washed with DI for 10 min to remove the cake layer, and the pure water flux was measured after 120 min and recorded as J_{WF2}. The flux recovery ratio (FRR) was obtained by Eq. (3):

$$FRR = \frac{J_{WF2}}{J_{WF}} \times 100 \tag{3}$$

Normally, membrane fouling is categorised based on the various forms of resistance that occur during the filtration process. To this end, Darcy's law was used to calculate the fouling resistances due to various mechanisms, as indicated in Eq. (4).

$$J_{WF} = \frac{\Delta P}{\mu \sum R} = \frac{\Delta P}{\mu R_t} \tag{4}$$

where ΔP, μ and $\sum R$ or R_t are the transmembrane pressure (Pa), viscosity of the permeate (Pa s), and total resistance (m^{-1}), respectively. The total membrane resistance generally combines the intrinsic membrane resistance (R_m) and fouling resistance (R_f). The intrinsic membrane resistance (R_m) can be calculated from Eq. (5).

$$R_m = \frac{\Delta P}{\mu J_{WF}} \tag{5}$$

Due to the difficulty of distinguishing fouling effects from concentration polarisation effects, these effects are combined and considered as membrane fouling effects [27]. This conceptualisation led to the assumption that R_f comprises the reversible fouling resistance (R_r) and the irreversible fouling resistance (R_{ir}), as indicated in Eqs. (6)–(9).

$$R_t = R_m + R_f = R_m + R_r + R_{ir} \tag{6}$$

$$R_{ir} = \frac{\Delta P}{\mu J_{WF2}} - R_m \tag{7}$$

$$R_f = \frac{\Delta P}{\mu J_{HA}} - R_m \tag{8}$$

$$R_r = R_f - R_{ir} \tag{9}$$

where R_f captures fouling and concentration polarisation effects.

3. Results and discussion

3.1. SEM analysis

Fig. 1 shows the surface images of the PES and PES/ZnO membranes. Inspection of these images revealed the formation of pore-like structures on the membrane surfaces. In this formation process, the size of these pores was varied in all of the ZnO/PES membranes. It is generally accepted that the addition of ZnO-NP to a membrane polymeric solution can increase the solution viscosity (Fig. 2) during phase separation. At a low ZnO-NP concentration in the membrane casting solution (less than 0.4 wt.%), the hydrophilicity effect is dominant, as reported elsewhere

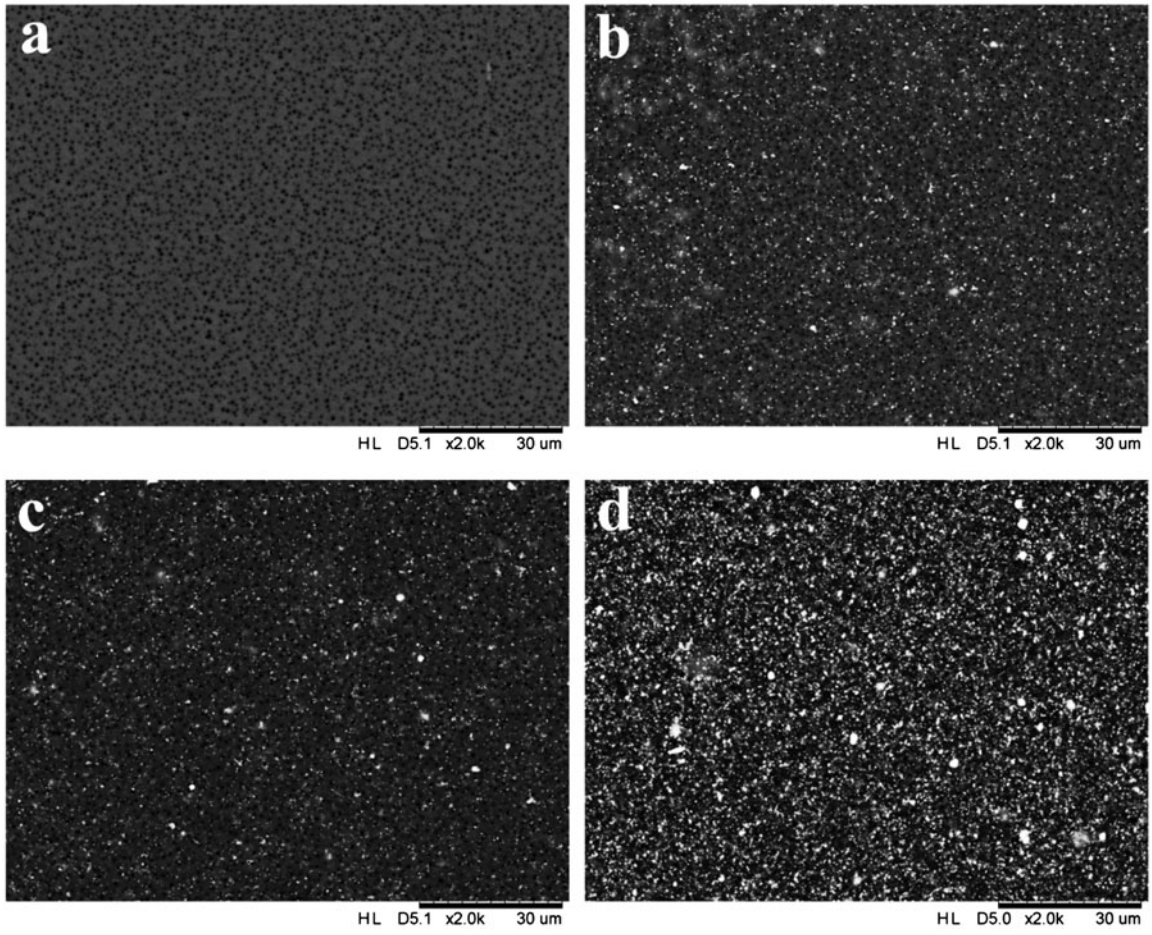

Fig. 1. SEM surface images of membranes prepared with different concentrations of ZnO: (a) 0 wt.%, (b) 1.25 wt.%, (c) 2.5 wt.% and (d) 3.75 wt.%.

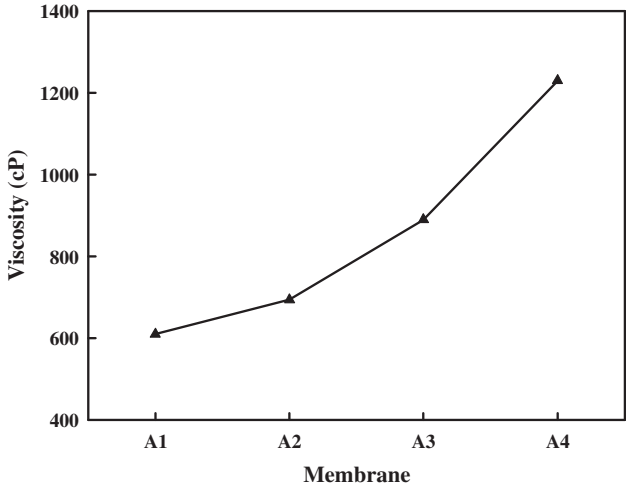

Fig. 2. The viscosity of casting dope solutions of A1, A2, A3 and A4 membranes.

[18]. However, at a low-polymer concentration and high-ZnO-NP concentration (more than 0.4 wt.%), the viscosity effect hinders polymer demixing during the phase separation. In addition, the ZnO-NP concentration used in this study was relatively high (>1 wt.%), which resulted in a notable difference between the viscosity of the pristine and that of the modified membranes. Moreover, it can be observed that the ZnO-NPs aggregated on the membrane surface, and the degree of aggregation was observed to increase with the ZnO content. This aggregation of the NPs on the membrane surface increased the probability of pore plugging, especially for the A3 and A4 membranes.

Cross-sectional SEM images of the prepared membranes are shown in Fig. 3. A comparison between the cross-sectional images of membranes prepared with different amounts of zinc oxide NPs indicate that all membranes possessed a finger-like structure. In addition, macrovoid formation was clearly enhanced as the ZnO-NP concentration increased. This enhancement

may logically be explained by the effect of the ZnO material added to the dope solution containing a low polymer concentration. The cast thickness of all membranes, before immersion in coagulation bath, is 200 μm (this is based on casting knife). The resulting membrane thickness was found to be thinner than the casting thickness. The difference in membranes' thickness is due to different degree of polymer densification after gelling. Similar observations were found by other researchers [28,29] during the fabrication of flat-sheet polymeric membranes.

3.2. Atomic force microscopy

Fig. 4 shows AFM surface images (1 × 1 μm) of membranes prepared with varying concentrations of ZnO-NPs in the casting solution. In these images, the dark areas indicate valleys and the brightest region represents the highest point of the membrane surface. The surface roughness parameters of the membranes were calculated by XEI data processing analysis software version 1.7.6 for a 5 × 5 μm scan size and are presented in Table 2. These results confirm that the roughness of the modified PES–ZnO membranes surface increased. Mainly, there are two important factors that indirectly affected on the membrane roughness; the PVP to ZnO-NPs ratio and the dope viscosity. For instance, at a concentration of 2.5 wt.% ZnO-NPs in the casting solution, there was a significant increase in the viscosity of the casting solution (Fig. 2). The high viscosity of the casting solution precluded the exchange between the solvent and the non-solvent (water), leading to the formation of a membrane with a smooth surface, smaller pores and denser structure, as demonstrated in Fig. 1(C) and Table 3.

However, it could be seen that A2 and A4 membranes possessed a higher roughness parameters than that of A3 membrane. In the case of A2 membrane, there was only (13%) increase in solution viscosity so the increase in roughness parameters is due to the presence of NPs in the dope solution (1.25%). In the case of A4 membrane, the solution viscosity was approximately double than that of pristine membrane. However, the increase in roughness parameters of this membrane might be due to low PVP to ZnO-NPs ratio. These conditions produced a rougher surface due to severe NPs aggregation on the membrane surface. Analogous trend had also been seen by other authors [30], when TiO_2 NPs loading increased to some extent. These changes in surface roughness parameters with NPs loading have also been observed by other workers during the preparation of mixed matrix membrane [9].

3.3. Contact-angle measurements

To assess the effect of ZnO-NPs on membrane hydrophilicity, the angle between a small droplet (2 μl) of water and the membrane surface was measured by a contact-angle instrument. The obtained results are shown in Fig. 5, which indicate that the addition of ZnO-NPs helped to improve the membrane hydrophilicity (decrease the contact angle) by approximately 6.29, 16.12 and 30.48% for the A2, A3 and A4 membranes, respectively. Additionally, there are two parameters that may have affected the contact angle; the hydrophilicity and the roughness of the membrane surface. As shown in Fig. 5, all of the PES/ZnO membrane samples exhibited a lower contact angle than that of the pristine PES membrane. Logically, this disparity in the contact-angle values between the pristine and the modified membranes could be attributed to the effect of the added ZnO-NPs. Physically, this phenomenon is manifested in the modified membranes due to the hydrophilicity of the added ZnO-NPs, which was interrupted within the membrane structure and possibly resulted in a membrane material with a higher affinity for water molecules. As explained previously in the section of AFM analysis, the A4 membrane showed the highest roughness parameters among all of the PES/ZnO membrane samples. The combined effects of hydrophilicity and roughness resulted in a low contact angle for the A4 membrane [31]. This phenomenon can be explained by Wenzel model [32]. In this model, it is stated that when a droplet of water is placed on the surface, it can follow the surface contours and roughness of the surface. In which, the degree of roughness could amplify either the hydrophilicity or the hydrophobicity of the surface as indicated in Eq. (10)

$$\cos\theta = r\cos\theta^{e} \tag{10}$$

where θ is apparent contact angle, θ^{e} is the contact angle on the flat surface and r is the roughness factor (the ratio of the actual solid/liquid contact area to its vertical projection). According to this model, r value represents the surface morphology and θ^{e} refer to the surface chemistry. Additionally, Kang et al. [33] also observed that the surface hydrophilicity/ hydrophobicity could be varied significantly by changing the surface roughness.

3.4. Membrane pore size

The average pore size of the PES and PES/ZnO membranes is listed in Table 3. It can be observed that there is a steady decrease in pore size due to the presence of the guest ZnO-NPs. This may be ascribed to the

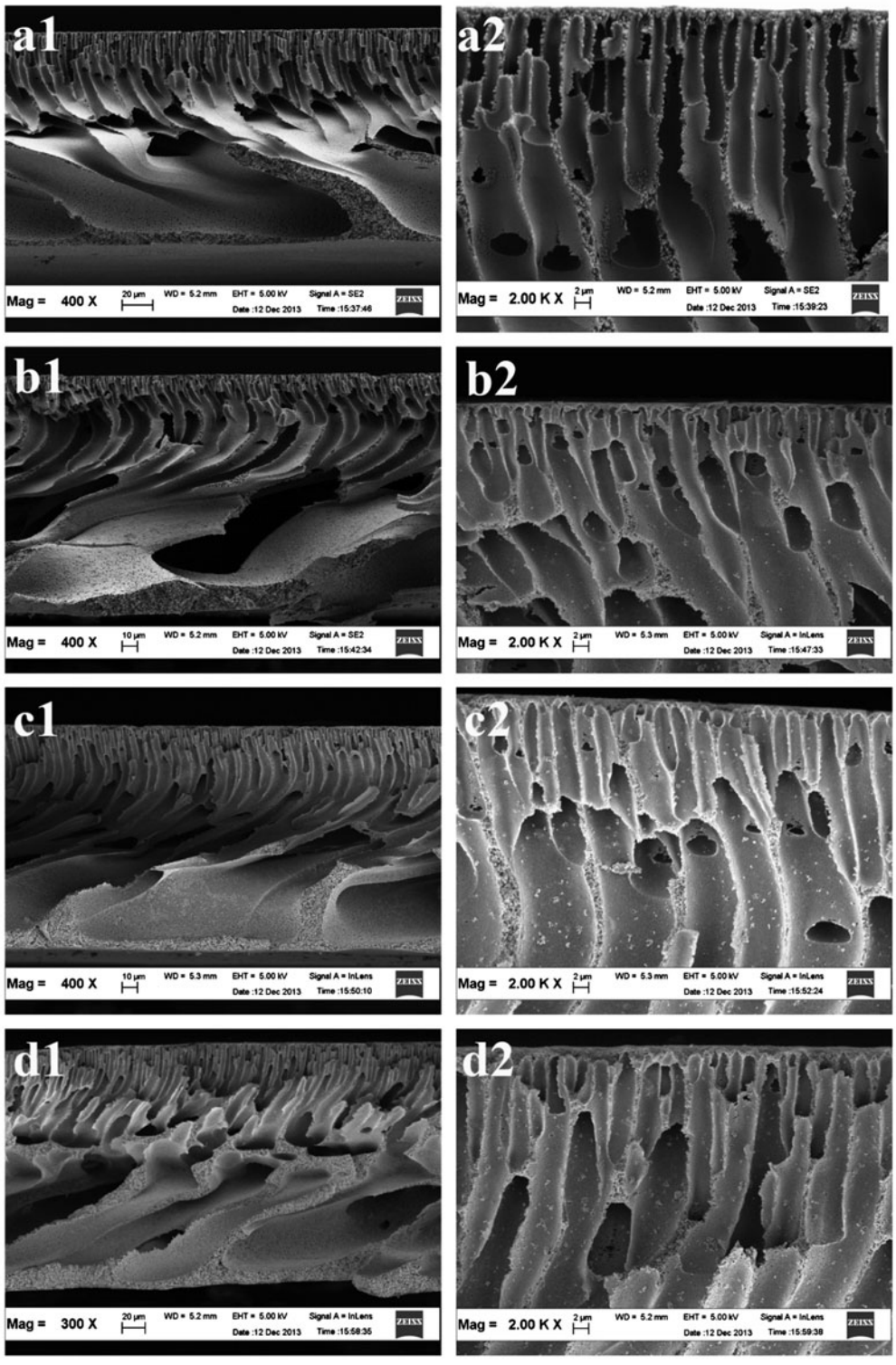

Fig. 3. SEM images of membranes prepared with different concentrations of ZnO-NPs: (1) cross-section; (2) skin layer; (a) 0 wt.% ZnO; (b) 1.25 wt.% ZnO; (c) 2.5 wt.% ZnO and (d) 3.75 wt.% ZnO.

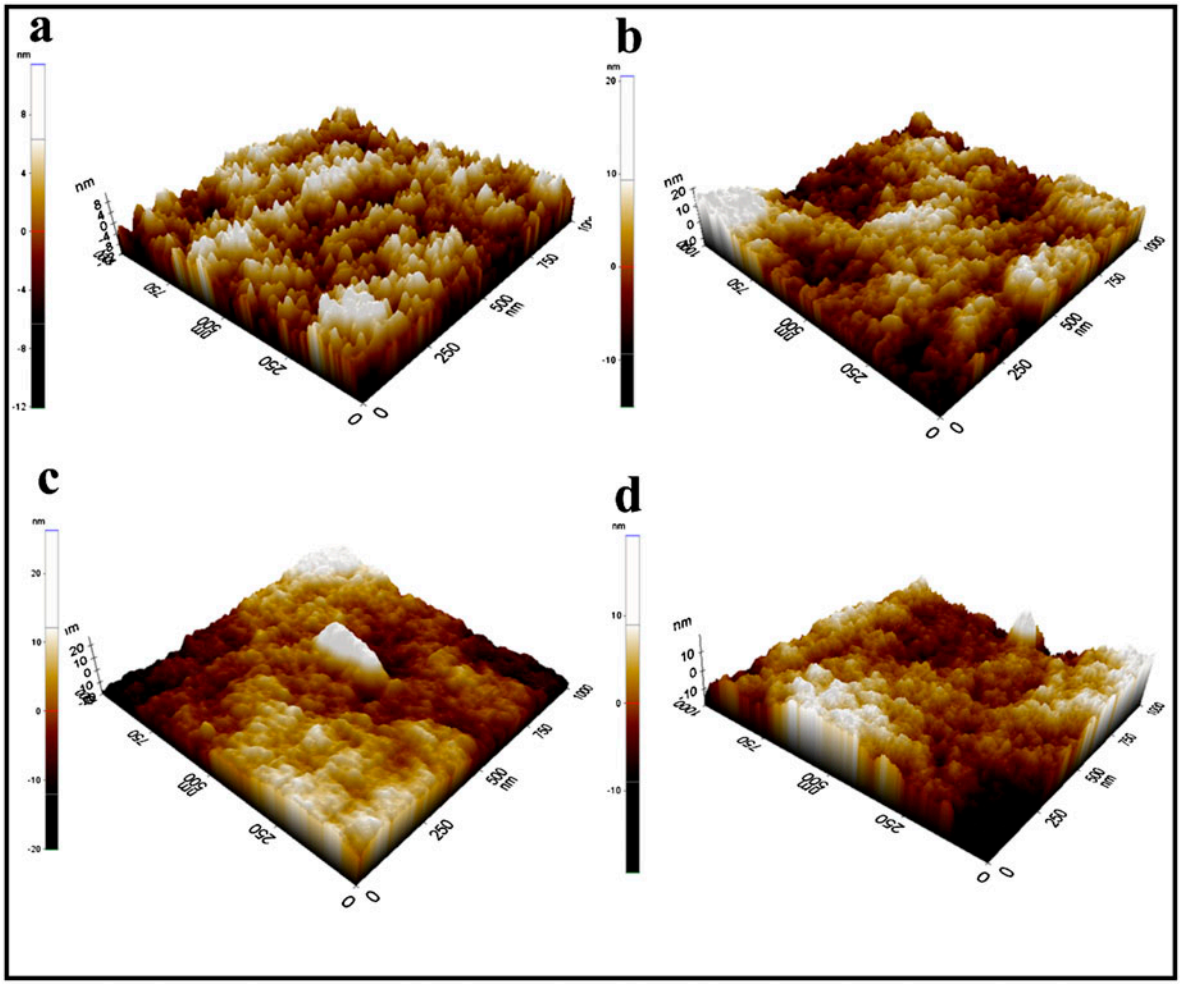

Fig. 4. Three-dimensional surface AFM images of membranes prepared with different concentrations of ZnO: (a) 0 wt.%, (b) 1.25 wt.%, (c) 2.5 wt.% and (d) 3.75 wt.%.

Table 2
Surface roughness parameters of PES/ZnO membranes

Membrane	R_q (nm)	R_a (nm)	R_z (nm)
A1	22.4	18.75	74.6
A2	41.16	32	139.3
A3	27.16	21.5	78.8
A4	47.8	38.4	144

Table 3
Pure water flux and pore size of PES/ZnO membranes

Membrane	PWF (L/m^2 h)	Pore size (nm)
A1	227.04	75
A2	317.45	72
A3	210.68	69
A4	180.44	63

decrease in the inter-diffusion rate during phase inversion (as also discussed in the SEM analysis). The obtained results are in good agreement with those obtained for the incorporation of analogous hydrophilic NPs into PES materials, as indicated in the literature [9].

3.5. Filtration performance

Table 3 summarises the average pure water fluxes (measured for three membrane samples). It can be clearly observed that the highest pure water flux was obtained at a ZnO concentration of 1.25 wt.% (A2 membrane). Over the A2 membrane, the recorded water flux was 317.45 L/m^2 h, which represents an improvement of 39.8% in membrane permeability relative to that of the pristine membrane (A1). This enhancement in membrane permeability was due to the improved membrane hydrophilicity (Fig. 5). Ngang et al. [34] found that the pore hydrophilization is playing an important factor for improving the permeability of mixed matrix

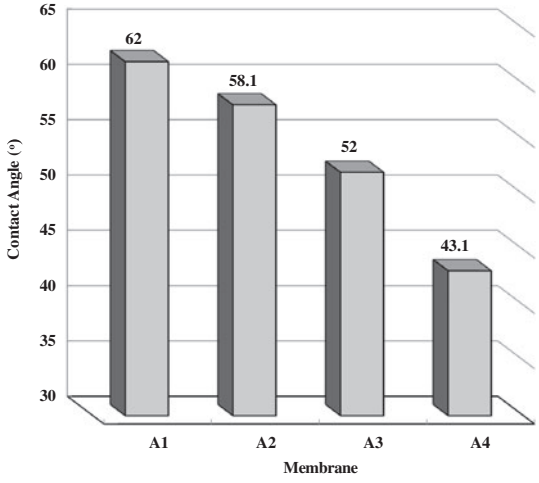

Fig. 5. The average contact angles on the top surface of A1, A2, A3 and A4 membranes.

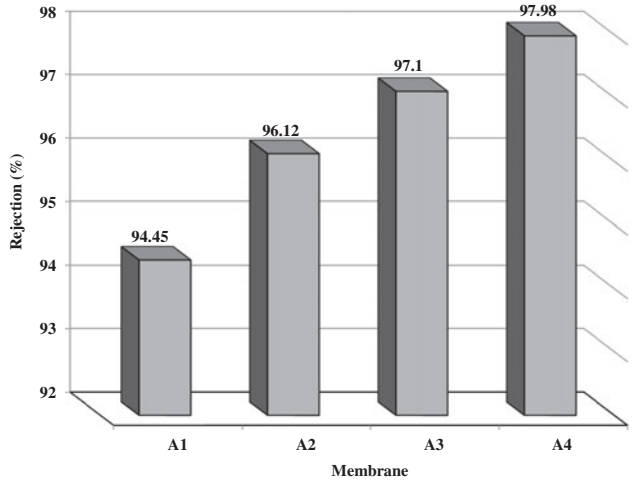

Fig. 6. Membrane rejection rates of A1, A2, A3 and A4 membranes.

membrane. In which, the hydrophilic NPs could form a hydroxyl group on membrane surface and pore wall that attract the water molecules to pass through the membrane. Vatanpour et al. [35] also observed that 1 wt.% of TiO_2 improved the membrane permeability by 31.1% over 5% increase in membrane pore size. This confirmed that the improved permeability of mixed matrix membrane-containing TiO_2 NPs is due to increase in both membrane pore size as well as hydrophilicity. However, other researchers believe that pore size plays the most important role in flux improvement [36,37]. The water flux was observed to decrease as the concentration of added ZnO exceeded 1.25 wt.%, which can be explained by the decrease in the pore size (as seen in Table 3).

Fig. 6 presents the rejection rates of the pristine PES and PES/ZnO membranes in filtering the HA solution. Two factors strongly affected the membrane performance: (i) membrane surface and sub-layer morphology and (ii) membrane surface properties, including hydrophilicity and roughness. As shown in the figure, all of the modified membranes exhibited a higher rejection rate than that of the pristine PES membrane (A1 membrane). This enhancement in the rejection rate exhibited by each membrane is in accordance with the decrease in pore size (Table 3) as a result of the addition of ZnO-NPs.

The normalised flux ratios (J_{HA}/J_{WF}) of all the prepared membranes are shown in Fig. 7. The flux ratios for the A1 and A2 membranes decreased rapidly during the first 30 min of HA filtration. After 30 min of HA filtration, there was a slight difference in the behaviour of the A3 and A4 membranes.

The maximum normalised flux ratios were achieved for the lowest-pore-size membranes (A3 and A4 membranes). These membranes were less prone to solute deposition, mainly because of the relatively smaller pores on the membrane surface (Table 3). A smaller membrane pore size prevents HA solutes from entering the pore length and thereby reduces the probability of pore blockage. In addition, the combined effect of the improved hydrophilicity and the low surface roughness was observed to play a key role in decreasing the fouling tendency of A3 membrane. These results and the conclusions drawn are in good standing with those of the pioneering study reported by Hamid et al. [1].

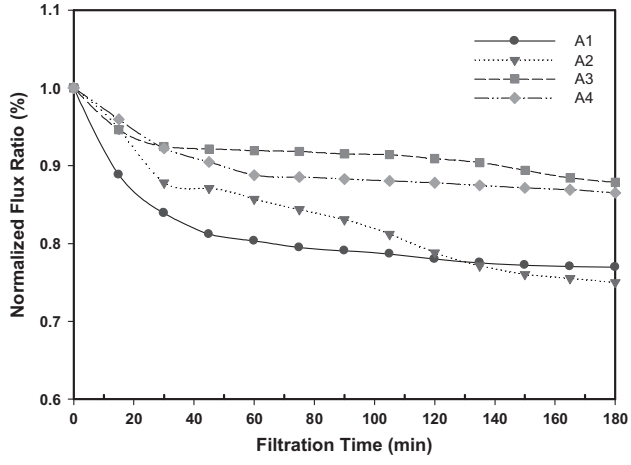

Fig. 7. Normalised flux ratios of A1, A2, A3 and A4 membranes.

3.6. Membrane fouling analysis

The most common way to investigate fouling mitigation on a membrane surface is via FRR. This technique can simply indicate the adsorption per cent of the foulant on a membrane surface (irreversible fouling). A high value of FRR indicates a strong resistance to membrane fouling. The FRR and the water fluxes due to various types of fouling mechanisms for all of the prepared membranes are presented in Table 4. Among all of the PES/ZnO-modified membranes, the A4 membrane showed the highest FRR.

To further investigate the membrane fouling resistance, a detailed analysis (as shown in Fig. 8) was performed in terms of intrinsic membrane resistance (R_m), which is related to membrane properties, total filtration resistance (R_t), reversible resistance (R_r) due to the attached foulant on the membrane surface and irreversible resistance (R_{ir}) due to the adsorption of a foulant on the membrane surface/pore surface, which were calculated using Eqs. (5)–(9).

It can be observed that among all of the intrinsic membrane resistances, the resistance of the A4 membrane was the highest, which may be explained by the fact that it possessed the smallest pore size among the prepared membranes. Also, this might be the result of NPs agglomeration, which leads to pore plugging and provides extra hydraulic resistance. However, the membrane resistance was the lowest for the A2 membrane, which was expected because the pure water flux was the highest for this membrane (Table 3).

Fig. 8 demonstrates that the fouling tendency for all of the membranes was lower than that of the pristine PES membrane. As mentioned previously, the fouling of the ZnO-modified membranes was enhanced mainly by the increased hydrophilicity and decreased roughness. However, the roughness parameters for all of the PES/ZnO membranes were greater than those of the PES membrane.

It is generally accepted that a membrane with smoother surface has more resistance to fouling [1]. The fouling tendency increased with roughness due to accumulating of solute (HA) in the "valleys" of the rough membrane surface. As indicated in Table 2, the roughness parameters of A2 and A4 membranes were increased and led to more reversible fouling resistance (R_r). While, the R_r for A3 membrane shows lowest value, this could be attributed to the smooth surface among the modified membranes. More investigation on Fig. 8 indicated that the R_{ir} of the prepared membranes decrease dramatically with ZnO content and reached to the lowest value of 1.89 for A4 membrane. This is mainly due to decrease in membrane pore size and improved hydrophilicity with more NPs loading. In fact, the pore size is the dominant factor that prevents the pore plugging by solute molecules in filtration process. At high membrane pore size, there will be a more solute penetration through the membrane pores and this leads to adsorption/deposition of the foulant onto pore surface. However, when there is a minor difference between the pore size of pristine and modified membranes, other factors owning the improvement of fouling resistance such as the hydrophilicity and surface roughness [1]. As indicated in Table 4 and Fig. 8 the pure water flux, HA solution flux and fouling resistance were enhanced due to the incorporation of ZnO-NPs into the PES membranes.

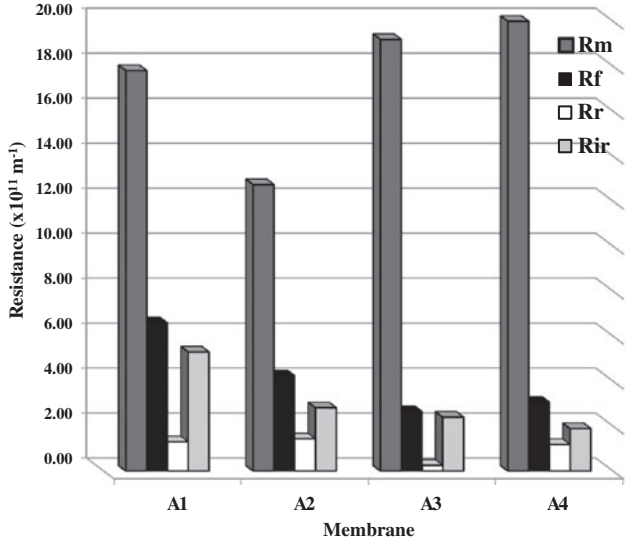

Fig. 8. Various types of filtration resistances of A1, A2, A3 and A4 membranes.

Table 4
Membrane fluxes due to different fouling mechanisms

Membrane	$J_{WF} \times 10^{-5}$ (m^3/m^2 s)	$J_{HF} \times 10^{-5}$ (m^3/m^2 s)	$J_{WF2} \times 10^{-5}$ (m^3/m^2 s)	FRR (%)
A1	6.29	4.59	4.85	77.08
A2	8.79	6.60	7.20	81.90
A3	5.84	5.13	5.19	88.90
A4	5.00	4.40	4.61	92.23

4. Conclusions

Dry/wet-phase inversion induced by the immersion precipitation technique was used to form membranes in this study. Due to the low PES concentration and relatively high ZnO concentration used, the dope viscosity increased with the addition of ZnO, which resulted in a

decrease in the pore size of the membranes obtained. It was observed that the addition of ZnO-NPs resulted in a reduction in the membrane's contact angle. Membrane performance analysis proved that the pure water flux and HA flux attained their ultimate values at the optimum concentration of 1.25 wt.% ZnO-NPs. The HA rejection rates were observed to increase with amount of ZnO-NPs added in the formulated membranes. Upon the addition of ZnO-NPs, the FRR of the ZnO-modified membranes was increased to 92.23%, which represented an improvement compared to the 77% recovery ratio obtained using the unmodified PES membrane. The irreversible fouling resistance was seen to decrease as the pore size decreased and hydrophilicity of the PES/ZnO membrane increased. The reversible fouling resistance was found to be affected by the surface hydrophilicity and roughness. As a result, the prepared PES/ZnO membranes demonstrated a reduction in HA fouling tendency and an improvement in the permeation flux.

Acknowledgements

The authors gratefully acknowledge the financial support of the MOSTI Science Fund (Grant no: 305/PJKIMIA/6013386), FRGS (Grant no: 203/PJKIMIA/6071234) and Universiti Sains Malaysia RU Membrane Cluster Science and Technology.

References

[1] N.A.A. Hamid, A.F. Ismail, T. Matsuura, A.W. Zularisam, W.J. Lau, E. Yuliwati, M.S. Abdullah, Morphological and separation performance study of polysulfone/titanium dioxide (PSF/TiO2) ultrafiltration membranes for humic acid removal, Desalination 273 (2011) 85–92.

[2] J.-J. Qin, M.H. Oo, Y. Li, Hollow fiber ultrafiltration membranes with enhanced flux for humic acid removal, J. Membr. Sci. 247 (2005) 119–125.

[3] P.C. Singer, Humic substances as precursors for potentially harmful disinfection by-products, Water Sci. Technol. 40 (1999) 25–30.

[4] G. Amy, J. Cho, Interactions between natural organic matter (NOM) and membranes: Rejection and fouling, Water Sci. Technol. 40 (1999) 131–139.

[5] I. Sutzkover-Gutman, D. Hasson, R. Semiat, Humic acid removal by deep-bed filtration and by UF membranes, Desalin. Water Treat. 31 (2011) 42–53.

[6] A.L. Ahmad, A.A. Abdulkarim, B.S. Ooi, S. Ismail, Recent development in additives modifications of polyethersulfone membrane for flux enhancement, Chem. Eng. J. 223 (2013) 246–267.

[7] F. Ma, H. Ye, Y.-Z. Zhang, X.-L. Ding, L.-G. Lin, L. Zhao, H. Li, The effect of polymer concentration and additives of cast solution on performance of polyethersulfone/sulfonated polysulfone blend nanofiltration membranes, Desalin. Water Treat. (2013) 1–8.

[8] S. Saedi, S.S. Madaeni, F. Seidi, A.A. Shamsabadi, S. Laki, Synthesis and application of a novel Amino-Starch derivative as a new polymeric additive for fixed facilitated transport of carbon dioxide through an asymmetric polyethersulfone (PES) membrane, Int. J. Greenhouse Gas Control 19 (2013) 126–137.

[9] A. Rahimpour, M. Jahanshahi, S. Khalili, A. Mollahosseini, A. Zirepour, B. Rajaeian, Novel functionalized carbon nanotubes for improving the surface properties and performance of polyethersulfone (PES) membrane, Desalination 286 (2012) 99–107.

[10] Q. Shi, Y. Su, S. Zhu, C. Li, Y. Zhao, Z. Jiang, A facile method for synthesis of pegylated polyethersulfone and its application in fabrication of antifouling ultrafiltration membrane, J. Membr. Sci. 303 (2007) 204–212.

[11] H. Wang, L. Yang, X. Zhao, T. Yu, Q. Du, Improvement of hydrophilicity and blood compatibility on polyethersulfone membrane by blending sulfonated polyethersulfone, Chin. J. Chem. Eng. 17 (2009) 324–329.

[12] A. Idris, I. Ahmed, M.A. Limin, Influence of lithium chloride, lithium bromide and lithium fluoride additives on performance of polyethersulfone membranes and its application in the treatment of palm oil mill effluent, Desalination 250 (2010) 805–809.

[13] A. Rahimpour, S.S. Madaeni, Y. Mansourpanah, Fabrication of polyethersulfone (PES) membranes with nano-porous surface using potassium perchlorate ($KClO_4$) as an additive in the casting solution, Desalination 258 (2010) 79–86.

[14] X. Cao, M. Tang, F. Liu, Y. Nie, C. Zhao, Immobilization of silver nanoparticles onto sulfonated polyethersulfone membranes as antibacterial materials, Colloids Surf., B 81 (2010) 555–562.

[15] H. Basri, A.F. Ismail, M. Aziz, K. Nagai, T. Matsuura, M.S. Abdullah, B.C. Ng, Silver-filled polyethersulfone membranes for antibacterial applications—Effect of PVP and TAP addition on silver dispersion, Desalination 261 (2010) 264–271.

[16] H. Basri, A.F. Ismail, M. Aziz, Polyethersulfone (PES)—silver composite UF membrane: Effect of silver loading and PVP molecular weight on membrane morphology and antibacterial activity, Desalination 273 (2011) 72–80.

[17] V. Vatanpour, S.S. Madaeni, A.R. Khataee, E. Salehi, S. Zinadini, H.A. Monfared, TiO2 embedded mixed matrix PES nanocomposite membranes: Influence of different sizes and types of nanoparticles on antifouling and performance, Desalination 292 (2012) 19–29.

[18] L. Shen, X. Bian, X. Lu, L. Shi, Z. Liu, L. Chen, Z. Hou, K. Fan, Preparation and characterization of ZnO/polyethersulfone (PES) hybrid membranes, Desalination 293 (2012) 21–29.

[19] L.C. Peng, W. Cathie Lee, A. Ahmad, A. Mohammad, Polysulfone membranes blended with ZnO nanoparticles for reducing fouling by oleic acid, Sep. Purif. Technol. 89 (2012) 51–56.

[20] J.F. Hernández-Sierra, F. Ruiz, D.C. Cruz Pena, F. Martínez-Gutiérrez, A.E. Martínez, A. de Jesús Pozos Guillén, H. Tapia-Pérez, G. Martínez Castañón, The antimicrobial sensitivity of *Streptococcus mutans* to nanoparticles of silver, zinc oxide, and gold, Nanomed. Nanotechnol. Biol. Med. 4 (2008) 237–240.

[21] A. Dodd, A. McKinley, M. Saunders, T. Tsuzuki, Effect of particle size on the photocatalytic activity of nanoparticulate zinc oxide, J. Nanopart. Res. 8 (2006) 43–51.
[22] I.A. Khattab, M.Y. Ghaly, L. Österlund, M.E.M. Ali, J.Y. Farah, F.M. Zaher, M.I. Badawy, Photocatalytic degradation of azo dye Reactive Red 15 over synthesized titanium and zinc oxides photocatalysts: a comparative study, Desalin. Water Treat. 48 (2012) 120–129.
[23] Y. Wang, L. Yang, G. Luo, Y. Dai, Preparation of cellulose acetate membrane filled with metal oxide particles for the pervaporation separation of methanol/methyl tert-butyl ether mixtures, Chem. Eng. J. 146 (2009) 6–10.
[24] S. Balta, A. Sotto, P. Luis, L. Benea, B. Van der Bruggen, J. Kim, A new outlook on membrane enhancement with nanoparticles: The alternative of ZnO, J. Membr. Sci. 389 (2012) 155–161.
[25] S. Anitha, B. Brabu, D.J. Thiruvadigal, C. Gopalakrishnan, T.S. Natarajan, Optical, bactericidal and water repellent properties of electrospun nano-composite membranes of cellulose acetate and ZnO, Carbohydr. Polym. 87 (2012) 1065–1072.
[26] H. Bai, Z. Liu, D.D. Sun, Hierarchical ZnO nanostructured membrane for multifunctional environmental applications, Colloids Surf., A: Physicochem. Eng. Aspects 410 (2012) 11–17.
[27] A. Rahimpour, S.S. Madaeni, Y. Mansourpanah, Nano-porous polyethersulfone (PES) membranes modified by acrylic acid (AA) and 2-hydroxyethylmethacrylate (HEMA) as additives in the gelation media, J. Membr. Sci. 364 (2010) 380–388.
[28] S. Yang, Z. Liu, Preparation and characterization of polyacrylonitrile ultrafiltration membranes, J. Membr. Sci. 222 (2003) 87–98.
[29] B.K. Chaturvedi, A.K. Ghosh, V. Ramachandhran, M.K. Trivedi, M.S. Hanra, B.M. Misra, Preparation, characterization and performance of polyethersulfone ultrafiltration membranes, Desalination 133 (2001) 31–40.
[30] J. Ahmad, M.B. Hågg, Polyvinyl acetate/titanium dioxide nanocomposite membranes for gas separation, J. Membr. Sci. 445 (2013) 200–210.
[31] Z. Yi, L.-P. Zhu, Y.-Y. Xu, Y.-F. Zhao, X.-T. Ma, B.-K. Zhu, Polysulfone-based amphiphilic polymer for hydrophilicity and fouling-resistant modification of polyethersulfone membranes, J. Membr. Sci. 365 (2010) 25–33.
[32] R.N. Wenzel, Resistance of solid surfaces to wetting by water, Ind. Eng. Chem. 28 (1936) 988–994.
[33] C. Kang, H. Lu, S. Yuan, D. Hong, K. Yan, B. Liang, Superhydrophilicity/superhydrophobicity of nickel micro-arrays fabricated by electroless deposition on an etched porous aluminum template, Chem. Eng. J. 203 (2012) 1–8.
[34] H.P. Ngang, B.S. Ooi, A.L. Ahmad, S.O. Lai, Preparation of PVDF–TiO_2 mixed-matrix membrane and its evaluation on dye adsorption and UV-cleaning properties, Chem. Eng. J. 197 (2012) 359–367.
[35] V. Vatanpour, S.S. Madaeni, A.R. Khataee, E. Salehi, S. Zinadini, H.A. Monfared, TiO_2 embedded mixed matrix PES nanocomposite membranes: Influence of different sizes and types of nanoparticles on antifouling and performance, Desalination 292 (2012) 19–29.
[36] A. Razmjou, J. Mansouri, V. Chen, The effects of mechanical and chemical modification of TiO_2 nanoparticles on the surface chemistry, structure and fouling performance of PES ultrafiltration membranes, J. Membr. Sci. 378 (2011) 73–84.
[37] J.-F. Li, Z.-L. Xu, H. Yang, L.-Y. Yu, M. Liu, Effect of TiO_2 nanoparticles on the surface morphology and performance of microporous PES membrane, Appl. Surf. Sci. 255 (2009) 4725–4732.